

# Differential maturation and subcellular localization of severe acute respiratory syndrome coronavirus surface proteins S, M and E

Beatrice Nal,<sup>1†</sup> Cheman Chan,<sup>1†</sup> Francois Kien,<sup>1</sup> Lewis Siu,<sup>1</sup>  
Jane Tse,<sup>1</sup> Kid Chu,<sup>1</sup> Jason Kam,<sup>1</sup> Isabelle Staropoli,<sup>2</sup>  
Bernadette Crescenzo-Chaigne,<sup>3</sup> Nicolas Escriou,<sup>3</sup>  
Sylvie van der Werf,<sup>3</sup> Kwok-Yung Yuen<sup>4</sup> and Ralf Altmeyer<sup>1</sup>

<sup>1</sup>HKU-Pasteur Research Centre, 8 Sassoon Road, Hong Kong, China

<sup>2,3</sup>Unité d'Immunologie Virale<sup>2</sup> and Unité de Génétique Moléculaire des Virus Respiratoires<sup>3</sup>,  
Institut Pasteur, 25 rue du Dr Roux, Paris, France

<sup>4</sup>Department of Microbiology, The University of Hong Kong, Hong Kong, China

## Correspondence

Beatrice Nal  
bnal@hkucc.hku.hk

Post-translational modifications and correct subcellular localization of viral structural proteins are prerequisites for assembly and budding of enveloped viruses. Coronaviruses, like the severe acute respiratory syndrome-associated virus (SARS-CoV), bud from the endoplasmic reticulum Golgi intermediate compartment. In this study, the subcellular distribution and maturation of SARS-CoV surface proteins S, M and E were analysed by using C-terminally tagged proteins. As early as 30 min post-entry into the endoplasmic reticulum, high-mannosylated S assembles into trimers prior to acquisition of complex *N*-glycans in the Golgi. Like S, M acquires high-mannose *N*-glycans that are subsequently modified into complex *N*-glycans in the Golgi. The *N*-glycosylation profile and the absence of *O*-glycosylation on M protein relate SARS-CoV to the previously described group 1 and 3 coronaviruses. Immunofluorescence analysis shows that S is detected in several compartments along the secretory pathway from the endoplasmic reticulum to the plasma membrane while M predominantly localizes in the Golgi, where it accumulates, and in trafficking vesicles. The E protein is not glycosylated. Pulse-chase labelling and confocal microscopy in the presence of protein translation inhibitor cycloheximide revealed that the E protein has a short half-life of 30 min. E protein is found in bright perinuclear patches colocalizing with endoplasmic reticulum markers. In conclusion, SARS-CoV surface proteins S, M and E show differential subcellular localizations when expressed alone suggesting that additional cellular or viral factors might be required for coordinated trafficking to the virus assembly site in the endoplasmic reticulum Golgi intermediate compartment.

Received 7 October 2004

Accepted 10 January 2005

## INTRODUCTION

Virus particle assembly and budding is the last step of the virus life-cycle. It requires correct folding and post-translational modifications of structural proteins and their precise subcellular localization at the virus budding site. Assembly and budding of the recently identified severe acute respiratory syndrome coronavirus, SARS-CoV, (Kuiken *et al.*, 2003; Peiris *et al.*, 2003) is a complex process that requires coordinated maturation and trafficking of the four structural proteins, the nucleocapsid (N), the Spike (S), the membrane (M) and the envelope (E) proteins. Little is known about SARS-CoV membrane proteins trafficking

and function. By analogy with other animal and human coronaviruses it is assumed that SARS-N protein forms a ribonucleoprotein complex with RNA, which buds into the membrane of an endoplasmic reticulum Golgi intermediate compartment (ERGIC) where the surface proteins S, M and E need to be located for virus budding.

Protein glycosylation is a highly regulated process that plays a fundamental role in membrane protein folding, oligomerization, sorting and transport by the intracellular machinery (Helenius & Aebi, 2001). The S protein is a 150–180 kDa highly glycosylated trimeric class I fusion protein (Bosch *et al.*, 2003; Delmas & Laude, 1990; Tripet *et al.*, 2004) responsible for receptor binding (Delmas *et al.*, 1992; Williams *et al.*, 1991; Yeager *et al.*, 1992), virus-membrane fusion and tissue tropism of coronaviruses

†These authors contributed equally to this work.

Supplementary material available in JGV Online.

(Laude *et al.*, 1993). The SARS-S protein can use angiotensin converting enzyme 2 (ACE2) to enter cells and elicits a neutralizing antibody response in animals (Li *et al.*, 2003; Simmons *et al.*, 2004; Wong *et al.*, 2004; Yang *et al.*, 2004a, b). In some coronaviruses, S is cleaved into subunits S1 and S2 by subtilisin endoproteases resulting in an increased fusogenic activity (de Haan *et al.*, 2004; Taguchi, 1993). M is a glycosylated hydrophobic protein with three transmembrane domains bearing *N*- or *O*-glycosylation site at the N terminus (de Haan *et al.*, 2003; Escors *et al.*, 2001b; Klumperman *et al.*, 1994). It is the most abundant protein in the virion and thought to play a key role in organizing particle assembly (de Haan *et al.*, 2000). When co-expressed, M and E proteins of several animal coronaviruses including transmissible gastroenteritis virus (TGEV; Baudoux *et al.*, 1998a), mouse hepatitis virus (MHV; Bos *et al.*, 1996; Vennema *et al.*, 1996) or infectious bronchitis virus (IBV; Lim & Liu, 2001) can form viral particles even in the absence of N or S protein. Although E is implicated in virus particle formation it is only found at low levels in particles (Corse & Machamer, 2000; Fischer *et al.*, 1998; Vennema *et al.*, 1996).

While the budding site of several coronaviruses has been localized at the ERGIC (Klumperman *et al.*, 1994), the viral surface proteins can be found in downstream compartments of the secretory pathway when expressed by the virus or alone: M localizes predominantly in the Golgi apparatus (Escors *et al.*, 2001a; Locker *et al.*, 1994, 1995; Machamer *et al.*, 1990, 1993; Swift & Machamer, 1991), and S is found along the secretory pathway and at the plasma membrane (de Haan *et al.*, 1999; Lontok *et al.*, 2004; Opstelten *et al.*, 1995), while E is detected in perinuclear regions, the ER and Golgi (Corse & Machamer, 2003; Lim & Liu, 2001; Raamsman *et al.*, 2000). Coronavirus proteins acquire modifications of their *N*-glycans in Golgi compartments, which might play an important role in the virus life-cycle. Indeed *N*-glycans of viral receptor binding proteins like S play a role in virus binding to lectin receptor DC-SIGN (dendritic cell-specific ICAM-grabbing non-integrin) on dendritic cells (Lin *et al.*, 2003; Lozach *et al.*, 2004) or shielding neutralizing epitopes from antibody recognition (Wei *et al.*, 2003). On the other hand the glycan attached to the M protein is implicated in interferon (IFN)- $\alpha$  induction and *in vivo* replicative capacity (Baudoux *et al.*, 1998b; de Haan *et al.*, 2003).

The present work describes the differential maturation, post-translational glycosylation profile and subcellular localization of human coronavirus, the SARS-CoV surface proteins S, M and E.

## METHODS

**Plasmid constructions.** SARS-M and -E cDNAs were cloned from the strain HKU-39849 isolated from a SARS case in Hong Kong (Peiris *et al.*, 2003; Tsang *et al.*, 2003), and amplified by PCR with primers containing *Bss*III and *Nsi*I adaptor sites. The DNA sequence encoding the M2-FLAG peptide (DYKDDDDK) was included within the reverse primers for in-frame fusion in the 3'

end (M forward primer: 5'-ATATGCGCGCATGGCAGACAACGGTACTATTACCGTTGAG-3'; M reverse primer: 5'-TTGCATGCATTTACTTGTTCATCGTCATCCTTGTAGTCATCCTGTACTAGCAAAGCAATATTGTTCG-3'; E forward primer: 5'-ATATGCGCGCATGTACTCATTTCGTTTCGGAAG-3'; E reverse primer: 5'-TTGCATGCATTTACTTGTTCATCGTCATCCTTGTAGTCATCGACCAGAAAGATCAGGAACTC-3'). SARS-M and E-FLAG PCR fragments were cloned into the pSFV1 vector (Invitrogen) resulting in plasmids pSFV-M-FLAG and pSFV-E-FLAG. SARS-S cDNA was obtained directly from the RNA extracted from a BAL specimen (#031589) from a SARS case of the Hanoi French Hospital, Vietnam. After reverse transcription, overlapping S cDNA fragments were produced by nested PCR and cloned in plasmid PCR 2.1-TOPO (Invitrogen) using the following primers: S/F1/+12350-21372 with S/R1/-/23518-23498 followed by S/F2/+12406-21426 with S/R2/-/23454-23435 for the 5'-proximal fragment, and S/F3/+123258-23277 with S/R3/-/25382-25363 followed by S/F4/+123322-23341 with S/R4/-/25348-25329 for the 3'-proximal fragment. A cDNA fragment representing the complete S gene sequence (nt 21406-25348) was next assembled from clones with overlapping S cDNA fragments harbouring the consensus protein sequence as deduced by direct sequencing of the amplicons from specimen #031589. The resulting plasmid TOP10F'-SARS-S was used as the source of S cDNA for subsequent cloning. SARS-S cDNA was amplified by PCR with primers containing *Bss*III and *Apal* adaptor sites. The DNA sequence encoding the M2-FLAG peptide was included within the reverse primer (forward primer: 5'-ATATGCGCGCATGTTTATTTCTTATTATTTCTTAC-3'; reverse primer: 5'-ATATGGGCCCAACCACATCGATTGTGTAATGTAATTTGACACCCTTGAGAAC-3'). Alternatively, for improved expression codon-optimized SARS-S DNA was produced using GeneOptimizer Technology (Geneart), with a FLAG sequence in-frame at the 3' end. S-FLAG was subcloned into pSFV1 vector resulting in plasmid pSFV-S-FLAG. SARS-S, -M and E-EGFP or ECFP (enhanced green or cyan fluorescent protein; BD Biosciences) constructs were also produced. *Cla*I-FLAG-*Apal* sequences from pSFV-S, M, E-FLAG constructs were replaced with EG/CFP fragments produced by PCR with *Cla*I and *Apal* sites-containing primers (forward primer: 5'-ATACATCGATATGGTGA-GCAAGGGCGAGGAG-3'; reverse primer: 5'-ATATGGGCCCTTACTTGTACAGCTCGTCC-3'). The pEYFP-Golgi plasmid construct encoding the Golgi targeting sequence of  $\beta$ -1,4-galactosyltransferase fused to EYFP (enhanced yellow FP) fluorescent tag was obtained from BD Biosciences.

**Cells, SFV expression vector and antibodies.** The baby hamster kidney (BHK)-21 cell line was cultured at 37 °C, 5% CO<sub>2</sub>, in Glasgow minimum essential medium (GMEM) medium, 5% fetal calf serum (FCS), 20 mM HEPES, 10% tryptone-phosphate broth, 100 U penicillin ml<sup>-1</sup>, 100  $\mu$ g streptomycin ml<sup>-1</sup>.

Recombinant defective SFV particles were made as described previously (Staropoli *et al.*, 2000). Briefly, plasmids pSFV-helper2, pSFV-S, -M, E-FLAG were linearized by *Spe*I, purified and *in vitro* transcribed using SP6 Cap-Scribe RNA polymerase (Roche). pSFV-helper2 and pSFV-S, -M or E-FLAG derived capped RNAs were mixed in equal amounts and electroporated into BHK-21 cells. After 24 h, the supernatant containing the recombinant SFV particles was harvested, and particles were purified and activated to infect BHK-21 cells.

The following antibodies and sera were used: SARS convalescent patient sera C0, SARS patient convalescent C1 to C7 and acute A1 to A7 sera (both provided by M. Peiris, Microbiology department, Hong Kong University); human normal sera N1 to N10 (Red Cross of Hong Kong, 1999-2000); horse radish peroxidase (HRP)- and fluorescein (FITC)-coupled mouse IgG1 anti-FLAG M2 monoclonal antibodies (mAbs) (Sigma); anti-human ACE2 ectodomain mouse

IgG2a mAbs (R&D system); anti-Erp72 rabbit polyclonal Abs (Stressgen), anti-ERGIC-53 mouse IgG1 mAbs (provided by P. Hauri, Dept of Pharmacology/Neurobiology, University of Basel, Switzerland), anti-58K mouse mAbs (Abcam). HRP- and FITC-coupled goat anti-mouse and anti-human IgG secondary Abs were obtained from Zymed.

**Pulse-chase analysis.** BHK-21 cells were starved at 37 °C for 30 min in methionine- and cysteine-free DMEM (Gibco-BRL), 12 h after transfection. Cells were pulse-labelled with 0.3 mCi (12.3 MBq) <sup>35</sup>S-labelled methionine and cysteine (Promix; Amersham Biosciences) at 37 °C for 10 min, washed with unlabelled methionine and cysteine containing GMEM (Gibco-BRL) with 2% FCS, followed by incubation with this medium without FCS at 37 °C for 30 min to 12 h chase times.

Reactions were stopped by rinsing cells with chilled PBS and incubation on ice. Cells were lysed with lysis buffer (20 mM Tris/HCl pH 7.5, 150 mM NaCl, 2 mM EDTA, 1% Triton X-100) containing 5 mM PMSF (Roche Applied Sciences), cells debris were cleared by centrifugation and supernatants were immunoprecipitated with anti-FLAG M2 agarose affinity gel according to manufacturer's protocol (Sigma). Immunoprecipitated proteins were mixed with sample loading buffer containing 50 mM DTT and separated by 4–20% (for E and M) or 4–12% (for S) SDS-PAGE. Images were acquired by exposure to phosphoimager (Molecular Imager Fx; Bio-Rad).

**Endoglycosidase H (EndoH) and peptide-N-glycosidase F sensitivity assays.** Immunoprecipitated radiolabelled S or M proteins were washed twice in PBS, denatured in 0.5% SDS and 1% β-mercaptoethanol at 100 °C for 5 min, and incubated overnight at 37 °C in 10 mM sodium phosphate buffer pH 5.8 containing EndoH (5 mU; Roche Applied Sciences) or pH 7.6 with 1.2% Triton X-100 containing peptide-N-glycosidase F (2 U; Roche Applied Sciences). Reactions were stopped with sample loading buffer containing 50 mM DTT.

**Flow cytometry analysis.** BHK-21 cells were detached 20 h post-infection (p.i.) using 2 mM EDTA in PBS, washed, and stained for 45 min at 4 °C with 1:50 dilution of SARS patient serum in PBS containing 3% goat serum (GS). After washing, cells were labelled with FITC-conjugated anti-human IgG Abs for 30 min and analysed using a FACSCalibur (BD Biosciences). Mean of fluorescence intensity (MFI) was measured after labelling with fluorochrome-conjugated Abs.

**ACE2 co-immunoprecipitation assay.** Recombinant S-FLAG or *E. coli* bacterial alkaline phosphatase (BAP)-FLAG (Sigma) proteins previously pre-adsorbed onto M2 affinity gel beads (Sigma) for 2 h at 4 °C were incubated with soluble recombinant ACE2 protein (R&D Systems) for 2 h at 4 °C. Beads were washed four times with lysis buffer (20 mM Tris/HCl pH 7.5, 150 mM NaCl, 2 mM EDTA, 1% Triton X-100). Precipitates were separated by SDS-PAGE, blotted and detected with HRP-conjugated mouse IgG2a anti-ACE2 ectodomain or mouse anti-FLAG M2 mAbs.

**Subcellular localization by fluorescence microscopy.** Cells were grown on coverslips, fixed 6–15 h p.i. in 4% paraformaldehyde (in PBS) for 15 min, incubated in 50 mM NH<sub>4</sub>Cl (in PBS) for 10 min at room temperature and permeabilized in 0.1% Triton X-100 (in PBS) for 5 min. Cells previously incubated for 30 min at room temperature in PBS containing 10% GS were labelled for 1 h with primary Abs in PBS containing 5% GS, washed and stained with dye-conjugated secondary Abs for 1 h. Coverslips were then washed and mounted on slides using Mowiol mounting medium containing DABCO (Sigma) prior to analysis by confocal microscopy (Bio-Rad Radiance 2100). For time-lapse microscopy on living cells, BHK-21 cells were grown on glass bottom microwell dishes (MatTek Corporation). Before analysis, culture medium was

changed to Hanks' balanced salts solution, 10 mM HEPES, 0.1 × Optimem buffer (Gibco-BRL). Living cells were analysed under an Axiovert 200M microscope related to the AxioVision system (Zeiss) and images were acquired with intervals of 10 s.

## RESULTS

### Expression of S, M and E as C-terminal fusion proteins with the FLAG peptide and fluorescent proteins

We analysed the expression, glycosylation maturation profile and kinetics of SARS-S, -M and -E surface proteins folding in mammalian cells. All three proteins were expressed as C-terminal fusion proteins with the FLAG peptide (Lozach *et al.*, 2003), the GFP, or EGFP or ECFP (Yang *et al.*, 1996) using the defective Semliki Forest virus system (Liljestrom & Garoff, 1991).

### SARS-S N-glycan modification and oligomerization

We performed metabolic labelling and pulse-chase experiments to analyse the maturation profile of the SARS-S protein, a 1255 aa protein that contains 23 putative N-glycosylation sites (Fig. 1). For pulse-chase experiments, mock controls are shown in Supplementary material, Fig. S1 (in JGV Online). S-FLAG protein is first detected as a monomer with the apparent molecular mass of 170 kDa [Fig. 1a (\*), 0 h of chase]. As shown by its sensitivity to EndoH, the 170 kDa protein is N-glycosylated in the ER with high-mannose N-glycans (Fig. 1b, 0 h of chase). At 0.5 h post-chase a second EndoH-resistant but peptide-N-glycosidase F (PNGaseF)-sensitive S with the apparent molecular mass of 180 kDa appears (○) (Fig. 1a, b). The EndoH resistance reflects the conversion of high-mannose to complex type N-glycans in the *cis* to medial Golgi. The 180 kDa protein signal increases over time while the 170 kDa protein band diminishes in intensity from 1 h post-chase but still remains detectable at 12 h. These results indicate that a significant portion of SARS-S is retained in the ER while protein undergoes an efficient maturation resulting in its release from the quality control machinery and exit from the ER.

High molecular mass forms of S, with an apparent molecular mass of ~600 kDa, can be detected as early as 30 min post-entry into the ER (Fig. 1c). A double band can be detected at 1 h post-chase (Fig. 1c, # and <), which likely corresponds to high-mannose and complex glycosylated S oligomers, respectively. This result suggests that high-mannose N-glycans on S oligomers have been modified to complex N-glycans. The majority of ~600 kDa forms of S dissociates into monomers under heating in non-reducing conditions, suggesting that S oligomers do not correspond to covalently linked aggregates but to correctly folded S-associated proteins (Supplementary Fig. S2 in JGV Online). Based on our results and previous data on coronavirus S proteins we conclude that SARS-S is a trimer.

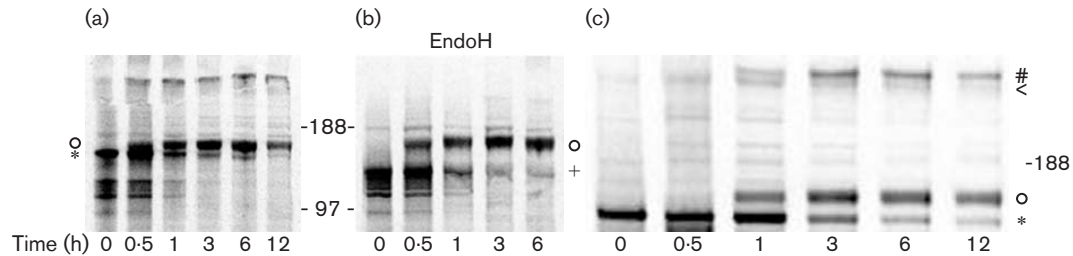


**Fig. 1.** SARS-S protein can mature into an EndoH resistant complex glycoform within 30 min following expression. BHK-21 cells were transfected with SARS-S encoding RNA and starved 12 h post-transfection at 37 °C for 30 min in methionine- and cysteine-free medium. Cells were pulse-labelled for 10 min in medium complemented with 0.3 mCi  $^{35}\text{S}$ -labelled methionine and cysteine amino acids and chased for increasing times before lysis. SARS-S proteins were immunoprecipitated from cell lysates with M2 mAb directed against the FLAG tag and analysed by SDS-PAGE and gel exposure to a phosphorimager screen. (a) Cells were chased for 0, 0.5, 1, 3, 6 and 12 h before harvest. (b) Cells were treated as in (a) and immunoprecipitated SARS-S was exposed to EndoH treatment. (c) Cells were treated as in (a) and immunoprecipitated SARS-S were run for longer time onto a SDS-PAGE to separate better SARS-S bands. \*, 170 kDa EndoH-sensitive S glycoform; O, 180 kDa EndoH-resistant S glycoform; +, 150 kDa EndoH-processed S glycoform; <, EndoH-sensitive S trimer; #, EndoH-resistant S trimer.

Additional protein species with molecular mass below 150 kDa were also detected by Western blotting, suggesting that they might be putative S1 and S2 subunits of S protein. In our pulse-chase experiments however these small proteins could only be detected at early time points and progressively disappeared after 30 min of chase. We therefore conclude that low molecular mass-proteins correspond to degradation products of misfolded SARS-S protein, which has not passed the ER quality control machinery.

### Purified recombinant SARS-S protein is recognized by SARS patient sera and binds soluble ACE2

In order to assess the correct folding of the recombinant SARS-S we analysed the recognition of cell surface-expressed S-FLAG by a panel of SARS patient sera and its binding capacity to the ACE2 receptor (Fig. 2). First, we used flow cytometry analysis to determine the efficiency of recognition of cell surface expressed S by human sera (Fig. 2a). We considered the value of geometric MFI, to evaluate serum reactivity. As a positive control, we tested a SARS patient serum (C0) that has previously been shown to be strongly reactive against S (Woo *et al.*, 2004). The MFI obtained for C0 serum was 98.5. All 11 convalescent SARS patient sera (C1 to C11) tested recognized cells expressing S with MFI ranging from 31.8 to 103.9 (mean value of 62.4). Eleven sera from normal blood donors were also tested and the mean value of MFI was 12.1. These data show that recombinant SARS-S is recognized by sera from convalescent SARS patients but not by sera from uninfected subjects.

ACE2 is a functional SARS-CoV receptor for virus entry (Li *et al.*, 2003; Wang *et al.*, 2004). We studied the interaction between immunopurified recombinant S-FLAG coated on Sepharose beads and purified soluble ACE2. Fig. 2(b) shows that recombinant SARS-S, but not a control

protein, BAP-FLAG, binds efficiently to the SARS-CoV receptor.

Altogether, these data suggest that the recombinant S produced in mammalian cells with the SFV expression system acquired a native-like fold that allows its recognition by SARS patient sera as well as binding to its physiological receptor ACE2.

### SARS-M protein is N-glycosylated

SARS-M is a 221 aa protein with a single potential N-glycosylation site and three potential O-glycosylation sites. Three major forms of M could be detected on SDS-PAGE after immunoprecipitation of extracts from pulse-labelled cells (Fig. 3a, see Supplementary Fig. S1 in JGV Online for mock control). The most abundant form of M migrates with an apparent molecular mass of 22 kDa (\*) and carries EndoH and PNGaseF-sensitive high-mannose N-glycans (Fig. 3b and c; 0, 0.5 and 1 h of chase). It is strongly detected until 1 h post-synthesis but only weakly at 3 h. The decrease in the 22 kDa M coincides with the gradual increase of a heterogeneous population of M protein migrating at 30–50 kDa (O) following 30 min post-synthesis. The 30–50 kDa protein forms carry complex N-glycans demonstrated by their resistance to EndoH (Fig. 3b) and sensitivity to PNGaseF (Fig. 3c). These results strongly indicate that the highly mannosylated 22 kDa M protein exits the ER and proceeds to the Golgi apparatus where it acquires modifications of its single N-glycan. Treatment of the 22 kDa or the 30–50 kDa M protein with O-glycosidase did not yield any band shift suggesting that SARS-M is not O-glycosylated (data not shown).

A stable protein of an apparent molecular mass of 18 kDa ( $\Delta$ ) was detected throughout the time course of the experiment. This protein did not undergo size shift and was

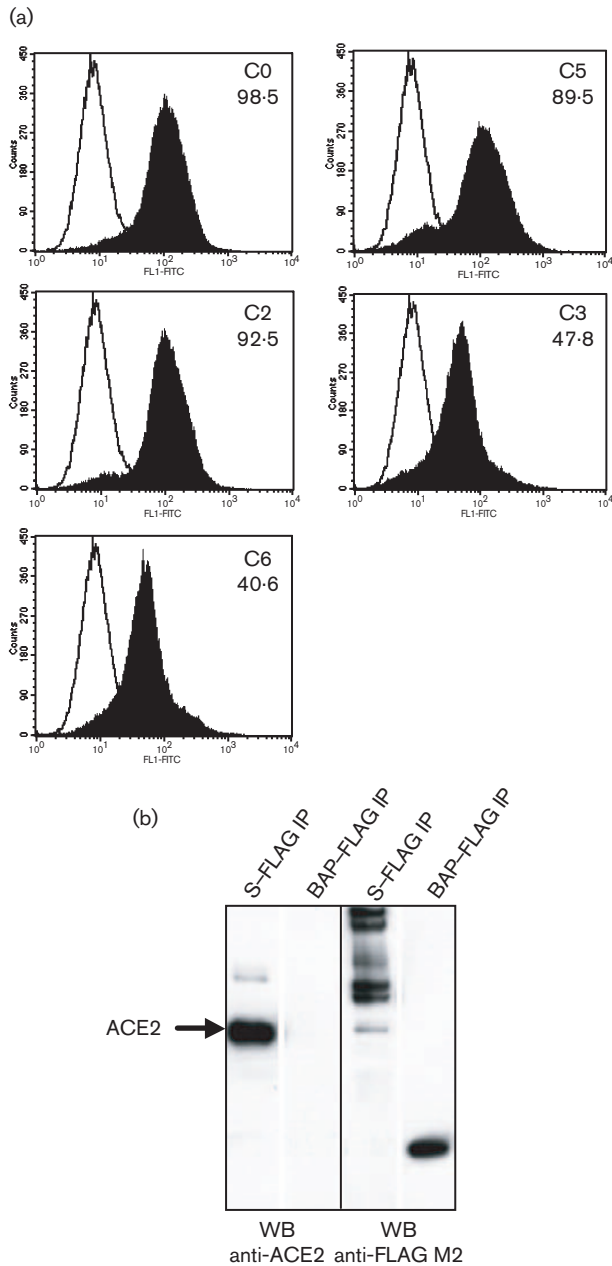


**Fig. 2.** Recombinant S is recognized by convalescent SARS patient sera and interacts with ACE2 *in vitro*. (a) SFV-S-infected BHK-21 cells were harvested 20 h p.i. and labelled with human sera (1:50), then detected with a goat secondary antibody anti-human IgG coupled to fluorescein (FITC). White histograms: normal human serum; black histograms: convalescent SARS-CoV-infected patient sera. C0: convalescent patient serum used as a positive control for S recognition; C2, C3, C5, C6: convalescent patient sera tested for S recognition. MFI are indicated for convalescent sera. (b) Soluble recombinant ACE2 protein was incubated with recombinant S-FLAG protein pre-adsorbed onto anti-FLAG M2 agarose affinity gel (S-FLAG IP). Recombinant *E. coli* BAP-FLAG protein was used as a negative control (BAP-FLAG IP). Precipitates were separated by SDS-PAGE followed by Western blot analysis with anti-ACE2 or anti-FLAG M2 mAbs.

not susceptible to EndoH, PNGaseF (Fig. 3b, c) or O-glycosidase treatment (data not shown) indicating that neither O- nor N-glycosylation sites on the 18 kDa M protein are used. Similar to S, polypeptides with a lower than the calculated molecular mass of M-FLAG could be immunoprecipitated at early time points (Fig. 3). Expression of these polypeptides decreased at 1 h post-synthesis and became undetectable at 3 h suggesting that they represent degradation products of misfolded M proteins, which did not pass the ER quality control.

### SARS-E is not glycosylated and is rapidly degraded

SARS-E is a small 76 aa protein without potential N-glycosylation sites. E-FLAG migrates on SDS-PAGE with an apparent molecular mass of 10 kDa as a doublet of two very close bands (Fig. 4, see Supplementary Fig. S1 for mock control). This indicates a potential post-translational modification of the protein. The doublet was only distinguishable in experiments performed with long runs of efficiently expressed E protein samples in SDS-PAGE. Time course pulse-chase labelling performed 12 h p.i. revealed that E-FLAG protein has a half-life of 30 min (determined by quantification of E signals after phosphoimager exposure, not shown). The protein disappears gradually 1 h post-synthesis and is only weakly detected at 6 h (Fig. 4). Analysis of culture supernatants by immunoprecipitation with anti-FLAG M2 mAbs or nuclei by immunofluorescence did not show any evidence of secretion or nuclear localization of E. We conclude that E has intrinsic properties leading to rapid degradation. Confocal microscopy analyses in the presence of cycloheximide further confirmed this conclusion (see below).

### SARS-S glycoprotein is detected along the secretory pathway

The subcellular localization of individually expressed SARS-S protein was studied in SFV-S-infected mammalian cells by immunofluorescence and confocal laser microscopy. We performed co-labelling studies with organelle markers by taking advantage of both S-FLAG and S-GFP fusion proteins that have similar distributions (Fig. 5). At 6 h p.i., when SFV-derived protein expression is still weak (Liljestrom & Garoff, 1991), S-FLAG showed a predominantly ER-restricted pattern which overlapped the ER-resident protein Erp72 staining. At 15 h p.i., in addition to its colocalization with Erp72, S-FLAG was also detected in distinct bright dots throughout the cytoplasm and at the plasma membrane. We analysed further whether S localized in the ERGIC or Golgi by co-labelling S-GFP-expressing cells with resident proteins of these organelles, ERGIC-53 and Golgi-58K, respectively. As shown in Fig. 5, at 12 h p.i. S-GFP was detected throughout the cytoplasm with an ER characteristic pattern as well as in brighter perinuclear patches which colocalized with Golgi-58K and partially with ERGIC-53 (Fig. 5).

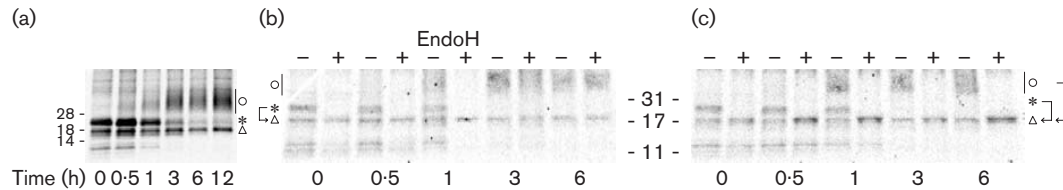


**Fig. 3.** SARS-M protein is *N*-glycosylated and matures within 30 min into an EndoH-resistant complex glycoform. BHK-21 cells were transfected with SARS-M encoding RNA and starved 12 h post-transfection at 37 °C for 30 min in methionine- and cysteine-free medium. Cells were pulse-labelled for 10 min with 0.3 mCi <sup>35</sup>S-labelled methionine and cysteine amino acids and chased for increasing times before cell lysis. SARS-M proteins were immunoprecipitated with M2 mAb directed against the FLAG tag and analysed by SDS-PAGE and phosphoimager screen exposure. (a) Cells were chased for 0, 0.5, 1, 3, 6 and 12 h before harvest. (b) Cells were treated as in (a) and immunoprecipitated SARS-M was exposed (+) or not (-) to EndoH treatment. An arrow on the left of the image shows the band shift caused by EndoH treatment. (c) Cells were treated as in (a) and immunoprecipitated SARS-M was exposed (+) or not (-) to peptide: *N*-glycosidase F (PNGaseF) treatment. Arrows on the right of the image show band shifts caused by PNGaseF treatment. Δ, Unglycosylated M form; \*, EndoH- and PNGaseF-sensitive M glycoform; ○, EndoH-resistant PNGaseF-sensitive M glycoform.

Our results show that, similarly to other coronaviruses, individually expressed recombinant SARS-S glycoproteins can be detected all along the secretory pathway of mammalian cells, from the ER to the plasma membrane.

### SARS-M glycoprotein localizes to the Golgi apparatus

M proteins of several coronaviruses accumulate in the Golgi complex of mammalian host cells. In order to analyse the subcellular localization of SARS-M we performed immunofluorescence analysis on BHK-21 cells expressing M-FLAG, M-ECFP or M-EGFP fusion proteins previously shown to have similar distributions (data not shown). At 6 h p.i., M proteins were exclusively concentrated in a perinuclear patch, which colocalizes with a Golgi marker (targeting sequence of the Golgi β-1,4-galactosyltransferase fused to EYFP fluorescent tag), but did not colocalize with the Erp72 ER marker (Fig. 6a, 6 h p.i.). When cells were analysed at 12 or 15 h p.i. (Fig. 6a and data not shown), a positive staining for M-EGFP clearly colocalized with

Golgi marker Golgi-58K in the perinuclear area and was also associated with distinct dots within the cytoplasm, (Fig. 6a, 12 h p.i.). Golgi localization was confirmed further by treatment of M-expressing cells with Brefeldin A (BFA), which induced the complete redistribution of M protein from the Golgi into the ER (Fig. 6a). M-EGFP partially colocalized with ERGIC marker, ERGIC-53, within the Golgi perinuclear area. Moreover, some of the dots positive for M labelling also merged with ERGIC-53 staining, suggesting the presence of ERGIC vesicles trafficking between ER and Golgi. To address better the question of M trafficking, we performed time-lapse microscopy experiments on living cells expressing M-EGFP (Fig. 6b). Interestingly, starting at 3.5 h p.i., we were able to follow M-EGFP protein expression, accumulation and trafficking in living cells. At shortest times, signal for M-EGFP was weak and only detectable in the Golgi apparatus (Fig. 6b, see Supplementary material in JGV Online to visualize the video sequence). Within a few minutes the signal became brighter showing a strong accumulation of M-EGFP in the Golgi apparatus. Parallel to the increase in M-EGFP expression, vesicles moving out of as well as vesicles moving towards the Golgi apparatus were detected, suggesting an important M trafficking phenomenon.

These results strongly argue for the accumulation of individually expressed SARS-M within the Golgi compartment and are consistent with our biochemical analyses showing that M acquires complex *N*-glycans in the Golgi. They also show that M protein is transported throughout the cytoplasm within trafficking vesicles moving towards and exiting the Golgi apparatus.

### SARS-E protein forms large membrane clusters co-distributing with ER markers

SARS-E protein localization was analysed at 6, 12 and 15 h p.i.. Fluorescence for E was identified as bright large spots colocalizing with the Erp72 ER marker (Fig. 7). However, in

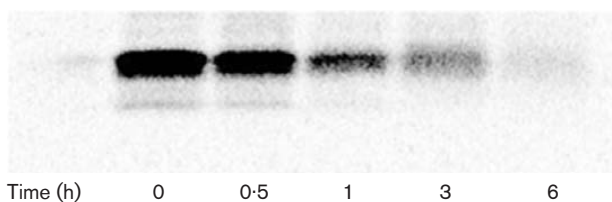


**Fig. 4.** SARS-E is degraded within 3 h post-synthesis. BHK-21 cells were transfected with SARS-E encoding RNA and starved 12 h post-transfection at 37 °C for 30 min in methionine- and cysteine-free medium. Then, cells were pulse-labelled for 10 min with medium containing 0.3 mCi <sup>35</sup>S-labelled methionine and cysteine amino acids and chased for 0–6 h before lysis, SARS-E immunoprecipitation with M2 anti-FLAG mAb SDS-PAGE and phosphoimager exposure.

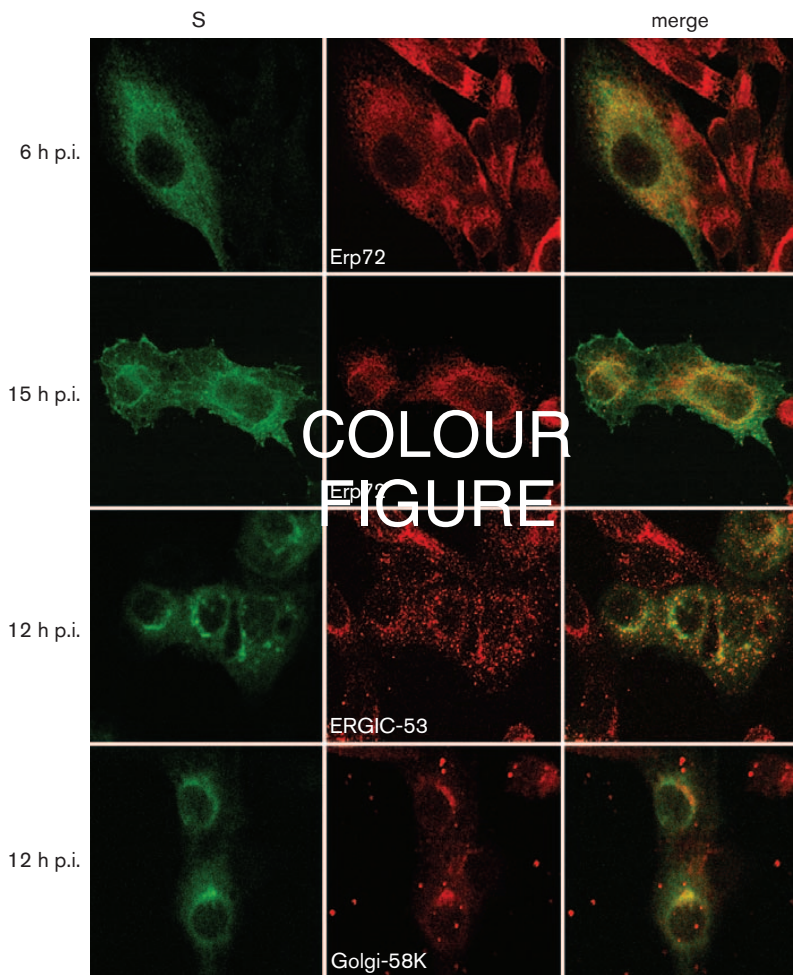


**Fig. 5.** SARS-S is localized along the secretory pathway from the ER to the plasma membrane. BHK-21 cells were grown on glass coverslips for 24 h preceding infection with recombinant SFV particles for (FLAG or GFP)-tagged S expression. Cells were harvested at indicated times p.i. and labelled with the corresponding antibodies. Erp72, ER marker; ERGIC-53, marker for the ER-Golgi intermediate compartment; Golgi-58K, Golgi marker.

contrast to SARS-S, -E did not distribute with a typical ER-type pattern. Furthermore, in E-expressing cells, Erp72 staining no longer appeared with a usual reticulated ER pattern. When E-expressing cells were treated for 1 or 3 h with cycloheximide, which inhibits all eukaryotic protein synthesis, E labelling was strongly reduced confirming our biochemical evidence that E has a short half-life (data not shown).

## DISCUSSION

Post-translational modifications, folding, oligomerization and cellular trafficking of viral structural proteins are keys to viral protein maturation and correct assembly of infectious virion particles. In this report, we used C-terminally tagged recombinant proteins to show that SARS-CoV surface proteins S, M and E present differential properties of expression, maturation kinetics, subcellular localization and stability, which could regulate viral protein assembly and virus budding.

In the present study, we show the SARS-S glycoprotein maturation kinetics, oligomerization, receptor binding and reactivity with SARS patient sera. Coronavirus S surface

proteins are highly glycosylated trimers (Luo *et al.*, 1999), which mediate virus entry through binding to specific cellular receptors (Delmas *et al.*, 1992; Williams *et al.*, 1991; Yeager *et al.*, 1992). SARS-S uses dendritic cell C-type lectin DC-SIGN for capture and transmission to target cells (Yang *et al.*, 2004b) and ACE2 for entry into host cells (Hofmann *et al.*, 2004a; Li *et al.*, 2003; Wang *et al.*, 2004; Wong *et al.*, 2004).

SARS-S protein contains 23 putative *N*-glycosylation sites, among which 12 have been described to be effectively glycosylated (Krokhin *et al.*, 2003; Ying *et al.*, 2004). Our data provide evidence that SARS-S protein, when expressed alone, acquires EndoH-resistant complex *N*-glycans in the Golgi within 30 min following expression. We detected both high-mannose and complex glycan *N*-glycoforms on S trimers within ER and Golgi, respectively. This result suggests that trimers form in the ER and pass the quality control to move towards the Golgi to acquire complex *N*-glycans. Proteolytic cleavage of surface glycoproteins by host proteases is required for viruses with class I fusion proteins, e.g. orthomyxoviruses, paramyxoviruses, retroviruses and filoviruses, to make the envelope fusogenic. Cleavage of MHV-S membrane glycoprotein into S1 and S2

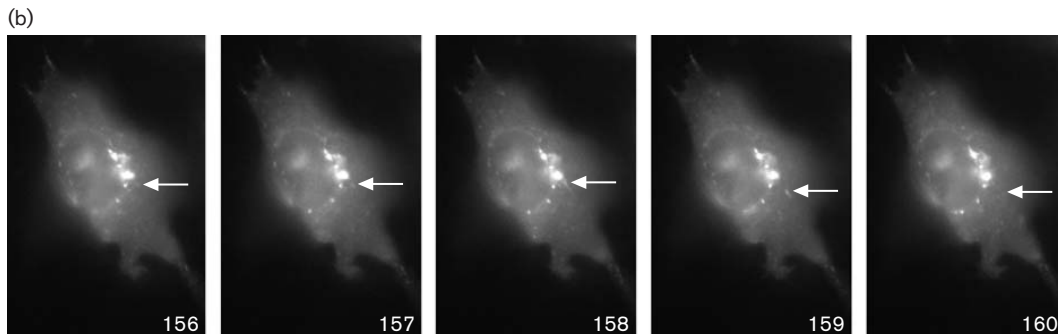
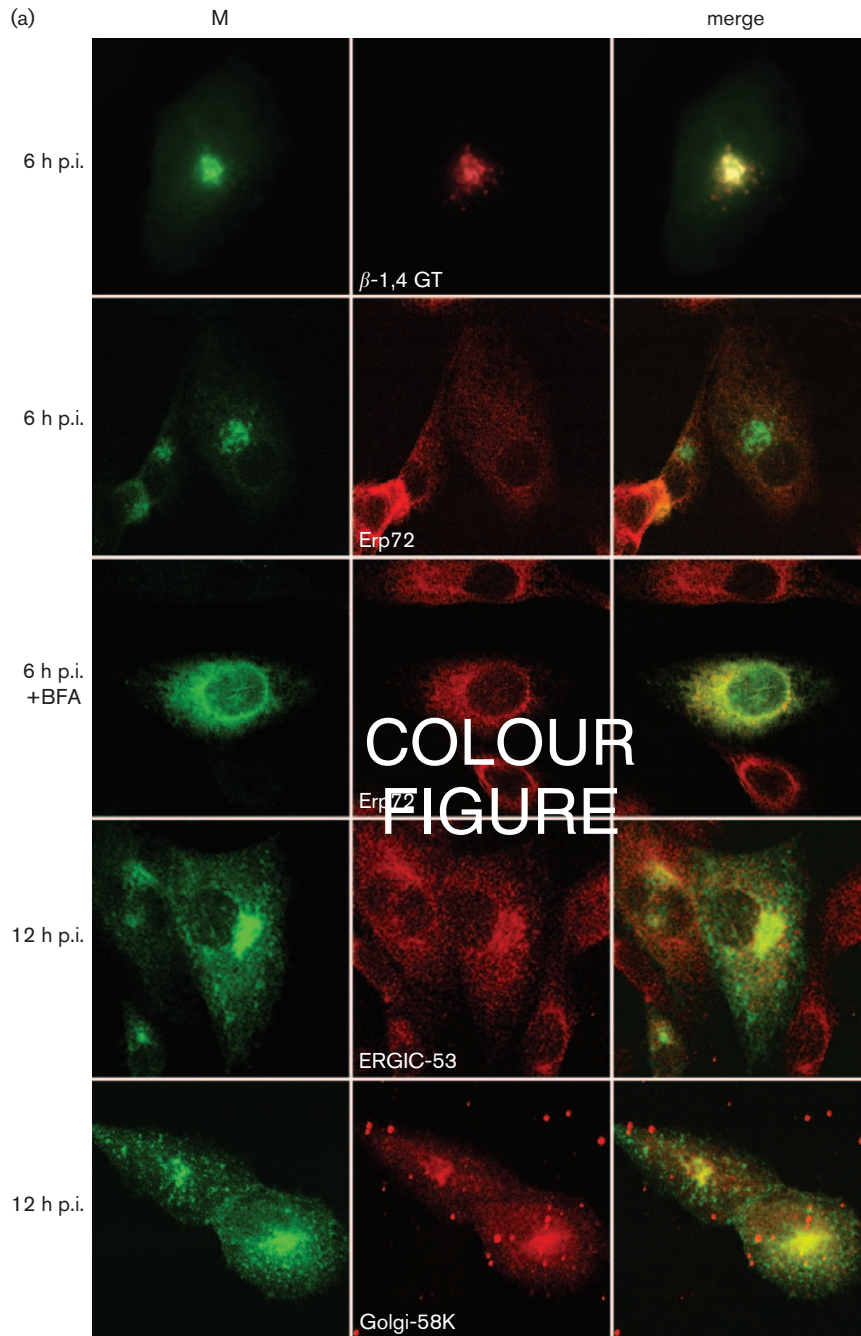


**Fig. 6.** SARS-M localizes within the Golgi apparatus and in trafficking vesicles throughout the cytoplasm. (a) Confocal microscopy experiments on BHK-21 cells expressing tagged SARS-M protein. BHK-21 cells were grown on glass coverslips. Upper panels: cells were transfected with a plasmid construct encoding a Golgi marker consisting in the targeting sequence of the Golgi  $\beta$ -1,4-galactosyltransferase (GT) fused to EYFP tag. All panels: cells were grown for 24 h prior to infection with recombinant SFV particles for (ECFP or FLAG)-tagged M expression. Cells were harvested at indicated times p.i. and labelled with the corresponding antibodies. Erp72, ER marker; ERGIC-53, marker for the ER-Golgi intermediate compartment; Golgi-58K, Golgi marker. (b) Time-lapse microscopy experiment on BHK-21 cells expressing M-EGFP. BHK-21 cells were grown on glass bottom microwell-Petri dishes for 24 h prior to infection with recombinant SFV particles for M-EGFP expression. Images were taken at 3.5 h p.i. and five snapshots out of a sequence of 550 are shown. Snapshot numbers are indicated at the bottom right side of each image and movements of trafficking vesicles out of the Golgi are indicated by arrows (see Supplementary material in JGV Online to visualize the video sequence).

subunits enhances fusion activity (de Haan *et al.*, 2004; Taguchi *et al.*, 1993), even if, depending on the MHV strain, MHV-S can be fusogenic without proteolytic cleavage (Taguchi, 1993). It was recently suggested that a  $\sim$ 100 kDa S protein fragment observed in recombinant His-tagged S-expressing cells might represent S2 subunit or cross-reacting bands (Simmons *et al.*, 2004; Xiao *et al.*, 2004). Although we also detected polypeptides with an apparent molecular mass close to the one expected for S2, they were found to be unstable in pulse-chase experiments suggesting that they represent degradation products of improperly folded S-protein precursors.

We show that SARS-S glycoprotein is present all along the secretory pathway from the ER to the plasma membrane. Our pulse-chase experiments combined with EndoH sensitivity assays show that although the majority of S had reached or passed through the Golgi, S could still be detected within the ER. Our results are in accordance with previous studies that described coronavirus S glycoprotein within the ER and at the cell surface. MHV-59 S glycoprotein has been observed predominantly in the ER with additional intense fluorescence in the Golgi perinuclear region where M localizes (Opstelten *et al.*, 1993). Recently, a C-terminal di-lysine motif in group 3 IBV coronaviruses and a di-basic motif in group 1 coronaviruses and SARS-CoV have been implicated in S localization within the ER

(Lontok *et al.*, 2004). SARS-S has also been shown at the cell surface by several groups where it mediates cell-to-cell fusion (Hofmann *et al.*, 2004b; Simmons *et al.*, 2004). We also observed a punctate SARS-S staining within the cytoplasm of expressing cells. An interesting issue would be to determine if these vesicles belong to the endosomal system. Correctly folded oligomeric SARS-S glycoprotein interacts with its entry receptor ACE2 *in vitro* and can be recognized by SARS patient sera. Previous studies showed that anti-S antibodies could neutralize virus infectivity (Buchholz *et al.*, 2004; Bukreyev *et al.*, 2004; Sui *et al.*, 2004; Xiao *et al.*, 2003; Yang *et al.*, 2004a). Purified SARS-S glycoprotein is therefore an ideal antigen to develop a safe vaccine against SARS-CoV, as well as a tool for serodiagnosis.

Coronavirus M protein is the most abundant structural protein at the surface of virus particles. In group 2 coronaviruses, e.g. MHV and human CoV-OC43 M is O-glycosylated while in group 1 and 3 coronaviruses, e.g. TGEV, FIPV and human CoV-229E M is N-glycosylated (Klumperman *et al.*, 1994; Niemann *et al.*, 1984; Stern & Sefton, 1982). M is both N- and O-glycosylated in IBV (Klumperman *et al.*, 1994). Here, we show that SARS-M protein is N- but not O-glycosylated in mammalian cells. Coronavirus M glycoprotein is responsible for the induction of IFN- $\alpha$  in leukocytes (Baudoux *et al.*, 1998a). Interestingly this interferogenic activity depends on the

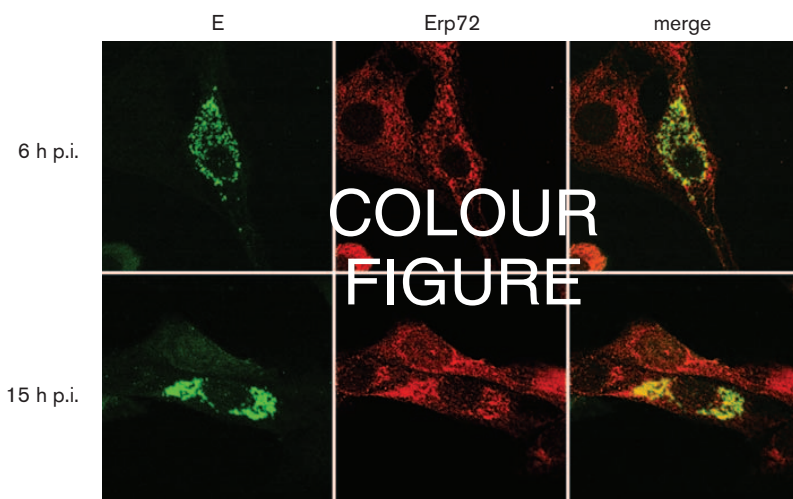


**Fig. 7.** Subcellular localization of SARS-E protein. BHK-21 cells were grown on glass coverslips for 24 h preceding infection with recombinant E-FLAG SFV particles. Cells were harvested at indicated times p.i. and labelled with antibodies against Erp72 ER marker and FLAG tag.

glycosylation status of M, with *N*-glycosylated M of MHV being more interferogenic than *O*- or un-glycosylated M (de Haan *et al.*, 2003). It is not known whether SARS-M protein induces IFN- $\alpha$  and whether high-mannose or complex glycans are involved in this process.

The ERGIC is the budding site for coronaviruses (Klumperman *et al.*, 1994). Individually expressed coronavirus M proteins have already been described to concentrate within the Golgi apparatus (Klumperman *et al.*, 1994; Locker *et al.*, 1992). Depending on the virus strain, the precise distribution of M differs, i.e. IBV- and MHV-M proteins are retained in *cis*- and *trans*-Golgi, respectively (Locker *et al.*, 1995; Machamer *et al.*, 1990; Swift & Machamer, 1991). Our data indicate that C-terminally tagged SARS-M glycoprotein strongly colocalizes with Golgi markers and partially with the ERGIC-53 protein, a lectin which cycles between ER, ERGIC and *cis*-Golgi (Appenzeller *et al.*, 1999). Mature SARS-M proteins carrying complex *N*-glycans may have to engage into retrograde transport from the Golgi apparatus to the ER or ERGIC in order to attain the budding site, phenomenon already described for MHV- and IBV-M (de Haan *et al.*, 2000; Maceyka & Machamer, 1997). Notably, time-lapse microscopy studies on living cells expressing SARS-M allowed us to identify vesicles, which traffic out of the Golgi compartment while no plasma membrane labelling was detected. Although we cannot exclude a Golgi retention defect caused by the C-terminal tag, other mechanisms are most likely responsible for this trafficking: M retrograde transport from Golgi to ER or M transport to the plasma membrane associated to highly efficient endocytosis and recycling.

Although E protein is only found at low levels in coronavirus envelope, it has a pivotal role in virus assembly (Corse & Machamer, 2000, 2002; Fischer *et al.*, 1998; Lim & Liu, 2001). Previous studies have demonstrated that the formation of virus-like particles solely depends on the co-expression of both M and E proteins (Vennema *et al.*, 1996). Here, we show that individually expressed SARS-E envelope protein has a half-life of 30 min and is no longer detectable at 6 h post-synthesis. A previous report showed that coronavirus MHV-E protein stability is comparable with that of the small envelope glycoprotein (Gs), a minor virion component of equine arteritis virus, which was found earlier to be prone to degradation (de Vries *et al.*, 1995; Raamsman *et al.*, 2000). Those data suggest that E could be regulated at a post-translational level. The mechanism involved in E degradation and the potential implication of this phenomenon in E protein level regulation remain unknown. The two close bands observed for SARS-E may correspond to a post-translational modification event. Based on the evidence that IBV-E protein has been shown to be palmitoylated (Corse & Machamer, 2002), albeit results differ in MHV and TGEV (Godet *et al.*, 1992; Raamsman *et al.*, 2000; Yu *et al.*, 1994), palmitoylation may occur in one or more of the three cysteine residues of SARS-E protein, which were predicted to be juxtamembranous

(Arbely *et al.*, 2004). Moreover, it was speculated that palmitoylation could play a role in the membrane curvature induction by SARS-E protein. Our immunofluorescence analysis shows that SARS-E protein concentrates in bright perinuclear clusters co-labelling with Erp72 ER marker. However, the distribution of Erp72 no longer displays its usual ER tubo-reticular profile when co-expressed with E. Consistently, MHV E has been described to have a peculiar punctate staining pattern by immunofluorescence and to induce the formation of electron-dense structures (Raamsman *et al.*, 2000). It was proposed that those structures consist of masses of tubular, smooth membranes with much curvature that are part of the ERGIC and form networks in continuity with the ER.

In this study, we used C-terminally tagged SARS-CoV viral proteins and we are confident, based on our observations, which corroborate anterior studies, that the tags did not influence SARS-S, -M and -E maturation steps and subcellular localizations.

Altogether, our findings are consistent with previous data on coronavirus S, M and E protein biogenesis, maturation process and subcellular distribution and establish a basis in understanding the intrinsic biochemical properties of SARS-CoV surface proteins. Future studies will have to address the issues of regulation of differential maturation and the role of viral proteins, the cellular partners and pathways underlying SARS-CoV assembly and budding.

## ACKNOWLEDGEMENTS

We would like to thank Lisa Chakrabarti and Spencer Shorte for help with videomicroscopy, George Tsao and Tony Chan for giving us access to the confocal microscope of the Anatomy Department of Hong Kong University, Peter Hauri for providing antibody to ERGIC-53, Malik Peiris for providing sera from SARS-CoV-infected patients, Jean-Claude Manuguerra for obtaining the specimen #031589, Frank Kunst for help with the design of S primers and Christiane Bouchier for help with sequencing of the S gene. Part of this work was funded by the Research Fund for Infectious Disease, Bureau of Health, Welfare and Food.

## REFERENCES

- Appenzeller, C., Andersson, H., Kappeler, F. & Hauri, H. P. (1999). The lectin ERGIC-53 is a cargo transport receptor for glycoproteins. *Nat Cell Biol* 1, 330–334.
- Arbely, E., Khattari, Z., Brotons, G., Akkawi, M., Salditt, T. & Arkin, I. T. (2004). A highly unusual palindromic transmembrane helical hairpin formed by SARS coronavirus E protein. *J Mol Biol* 341, 769–779.
- Baudoux, P., Carrat, C., Besnardeau, L., Charley, B. & Laude, H. (1998a). Coronavirus pseudoparticles formed with recombinant M and E proteins induce alpha interferon synthesis by leukocytes. *J Virol* 72, 8636–8643.
- Baudoux, P., Besnardeau, L., Carrat, C., Rottier, P., Charley, B. & Laude, H. (1998b). Interferon alpha inducing property of coronavirus particles and pseudoparticles. *Adv Exp Med Biol* 440, 377–386.

- Bos, E. C., Luytjes, W., van der Meulen, H. V., Koerten, H. K. & Spaan, W. J. (1996).** The production of recombinant infectious DI-particles of a murine coronavirus in the absence of helper virus. *Virology* **218**, 52–60.
- Bosch, B. J., van der Zee, R., de Haan, C. A. & Rottier, P. J. (2003).** The coronavirus spike protein is a class I virus fusion protein: structural and functional characterization of the fusion core complex. *J Virol* **77**, 8801–8811.
- Buchholz, U. J., Bukreyev, A., Yang, L., Lamirande, E. W., Murphy, B. R., Subbarao, K. & Collins, P. L. (2004).** Contributions of the structural proteins of severe acute respiratory syndrome coronavirus to protective immunity. *Proc Natl Acad Sci U S A* **101**, 9804–9809.
- Bukreyev, A., Lamirande, E. W., Buchholz, U. J., Vogel, L. N., Elkins, W. R., St Claire, M., Murphy, B. R., Subbarao, K. & Collins, P. L. (2004).** Mucosal immunisation of African green monkeys (*Cercopithecus aethiops*) with an attenuated parainfluenza virus expressing the SARS coronavirus spike protein for the prevention of SARS. *Lancet* **363**, 2122–2127.
- Corse, E. & Machamer, C. E. (2000).** Infectious bronchitis virus E protein is targeted to the Golgi complex and directs release of virus-like particles. *J Virol* **74**, 4319–4326.
- Corse, E. & Machamer, C. E. (2002).** The cytoplasmic tail of infectious bronchitis virus E protein directs Golgi targeting. *J Virol* **76**, 1273–1284.
- Corse, E. & Machamer, C. E. (2003).** The cytoplasmic tails of infectious bronchitis virus E and M proteins mediate their interaction. *Virology* **312**, 25–34.
- de Haan, C. A., Smeets, M., Vernooij, F., Vennema, H. & Rottier, P. J. (1999).** Mapping of the coronavirus membrane protein domains involved in interaction with the spike protein. *J Virol* **73**, 7441–7452.
- de Haan, C. A., Vennema, H. & Rottier, P. J. (2000).** Assembly of the coronavirus envelope: homotypic interactions between the M proteins. *J Virol* **74**, 4967–4978.
- de Haan, C. A., de Wit, M., Kuo, L., Montalto-Morrison, C., Haagmans, B. L., Weiss, S. R., Masters, P. S. & Rottier, P. J. (2003).** The glycosylation status of the murine hepatitis coronavirus M protein affects the interferogenic capacity of the virus in vitro and its ability to replicate in the liver but not the brain. *Virology* **312**, 395–406.
- de Haan, C. A., Stadler, K., Godeke, G. J., Bosch, B. J. & Rottier, P. J. (2004).** Cleavage inhibition of the murine coronavirus spike protein by a furin-like enzyme affects cell-cell but not virus-cell fusion. *J Virol* **78**, 6048–6054.
- Delmas, B. & Laude, H. (1990).** Assembly of coronavirus spike protein into trimers and its role in epitope expression. *J Virol* **64**, 5367–5375.
- Delmas, B., Gelfi, J., L'Haridon, R., Vogel, L. K., Sjostrom, H., Noren, O. & Laude, H. (1992).** Aminopeptidase N is a major receptor for the entero-pathogenic coronavirus TGEV. *Nature* **357**, 417–420.
- de Vries, A. A., Raamsman, M. J., van Dijk, H. A., Horzinek, M. C. & Rottier, P. J. (1995).** The small envelope glycoprotein (G<sub>S</sub>) of equine arteritis virus folds into three distinct monomers and a disulfide-linked dimer. *J Virol* **69**, 3441–3448.
- Escors, D., Ortego, J. & Enjuanes, L. (2001a).** The membrane M protein of the transmissible gastroenteritis coronavirus binds to the internal core through the carboxy-terminus. *Adv Exp Med Biol* **494**, 589–593.
- Escors, D., Camafeita, E., Ortego, J., Laude, H. & Enjuanes, L. (2001b).** Organization of two transmissible gastroenteritis coronavirus membrane protein topologies within the virion and core. *J Virol* **75**, 12228–12240.
- Fischer, F., Stegen, C. F., Masters, P. S. & Samsonoff, W. A. (1998).** Analysis of constructed E gene mutants of mouse hepatitis virus confirms a pivotal role for E protein in coronavirus assembly. *J Virol* **72**, 7885–7894.
- Godet, M., L'Haridon, R., Vautherot, J. F. & Laude, H. (1992).** TGEV corona virus ORF4 encodes a membrane protein that is incorporated into virions. *Virology* **188**, 666–675.
- Helenius, A. & Aebi, M. (2001).** Intracellular functions of N-linked glycans. *Science* **291**, 2364–2369.
- Hofmann, H., Geier, M., Marzi, A., Krumbiegel, M., Peipp, M., Fey, G. H., Gramberg, T. & Pohlmann, S. (2004a).** Susceptibility to SARS coronavirus S protein-driven infection correlates with expression of angiotensin converting enzyme 2 and infection can be blocked by soluble receptor. *Biochem Biophys Res Commun* **319**, 1216–1221.
- Hofmann, H., Hattermann, K., Marzi, A. & 7 other authors (2004b).** S protein of severe acute respiratory syndrome-associated coronavirus mediates entry into hepatoma cell lines and is targeted by neutralizing antibodies in infected patients. *J Virol* **78**, 6134–6142.
- Klumperman, J., Locker, J. K., Meijer, A., Horzinek, M. C., Geuze, H. J. & Rottier, P. J. (1994).** Coronavirus M proteins accumulate in the Golgi complex beyond the site of virion budding. *J Virol* **68**, 6523–6534.
- Krokhin, O., Li, Y., Andonov, A. & 13 other authors (2003).** Mass spectrometric characterization of proteins from the SARS virus: a preliminary report. *Mol Cell Proteomics* **2**, 346–356.
- Kuiken, T., Fouchier, R. A., Schutten, M. & 19 other authors (2003).** Newly discovered coronavirus as the primary cause of severe acute respiratory syndrome. *Lancet* **362**, 263–270.
- Laude, H., Van Reeth, K. & Pensaert, M. (1993).** Porcine respiratory coronavirus: molecular features and virus-host interactions. *Vet Res* **24**, 125–150.
- Li, W., Moore, M. J., Vasilieva, N. & 9 other authors (2003).** Angiotensin-converting enzyme 2 is a functional receptor for the SARS coronavirus. *Nature* **426**, 450–454.
- Liljestrom, P. & Garoff, H. (1991).** A new generation of animal cell expression vectors based on the Semliki Forest virus replicon. *Biotechnology (N Y)* **9**, 1356–1361.
- Lim, K. P. & Liu, D. X. (2001).** The missing link in coronavirus assembly. Retention of the avian coronavirus infectious bronchitis virus envelope protein in the pre-Golgi compartments and physical interaction between the envelope and membrane proteins. *J Biol Chem* **276**, 17515–17523.
- Lin, G., Simmons, G., Pohlmann, S. & 8 other authors (2003).** Differential N-linked glycosylation of human immunodeficiency virus and Ebola virus envelope glycoproteins modulates interactions with DC-SIGN and DC-SIGNR. *J Virol* **77**, 1337–1346.
- Locker, J. K., Rose, J. K., Horzinek, M. C. & Rottier, P. J. (1992).** Membrane assembly of the triple-spanning coronavirus M protein. Individual transmembrane domains show preferred orientation. *J Biol Chem* **267**, 21911–21918.
- Locker, J. K., Klumperman, J., Oorschot, V., Horzinek, M. C., Geuze, H. J. & Rottier, P. J. (1994).** The cytoplasmic tail of mouse hepatitis virus M protein is essential but not sufficient for its retention in the Golgi complex. *J Biol Chem* **269**, 28263–28269.
- Locker, J. K., Opstelten, D. J., Ericsson, M., Horzinek, M. C. & Rottier, P. J. (1995).** Oligomerization of a trans-Golgi/trans-Golgi network retained protein occurs in the Golgi complex and may be part of its retention. *J Biol Chem* **270**, 8815–8821.
- Lontok, E., Corse, E. & Machamer, C. E. (2004).** Intracellular targeting signals contribute to localization of coronavirus spike proteins near the virus assembly site. *J Virol* **78**, 5913–5922.

- Lozach, P. Y., Lortat-Jacob, H., de Lacroix de Lavalette, A. & 9 other authors (2003). DC-SIGN and L-SIGN are high affinity binding receptors for hepatitis C virus glycoprotein E2. *J Biol Chem* **278**, 20358–20366.
- Lozach, P. Y., Amara, A., Bartosch, B., Virelizier, J. L., Arenzana-Seisdedos, F., Cosset, F. L. & Altmeyer, R. (2004). C-type lectins L-SIGN and DC-SIGN capture and transmit infectious hepatitis C virus pseudotype particles. *J Biol Chem* **279**, 32035–32045.
- Luo, Z., Matthews, A. M. & Weiss, S. R. (1999). Amino acid substitutions within the leucine zipper domain of the murine coronavirus spike protein cause defects in oligomerization and the ability to induce cell-to-cell fusion. *J Virol* **73**, 8152–8159.
- Maceyka, M. & Machamer, C. E. (1997). Ceramide accumulation uncovers a cycling pathway for the *cis*-Golgi network marker, infectious bronchitis virus M protein. *J Cell Biol* **139**, 1411–1418.
- Machamer, C. E., Mentone, S. A., Rose, J. K. & Farquhar, M. G. (1990). The E1 glycoprotein of an avian coronavirus is targeted to the *cis* Golgi complex. *Proc Natl Acad Sci U S A* **87**, 6944–6948.
- Machamer, C. E., Grim, M. G., Esqueda, A., Chung, S. W., Rolls, M., Ryan, K. & Swift, A. M. (1993). Retention of a *cis* Golgi protein requires polar residues on one face of a predicted  $\alpha$ -helix in the transmembrane domain. *Mol Biol Cell* **4**, 695–704.
- Niemann, H., Geyer, R., Klenk, H. D., Linder, D., Stirm, S. & Wirth, M. (1984). The carbohydrates of mouse hepatitis virus (MHV) A59: structures of the O-glycosidically linked oligosaccharides of glycoprotein E1. *EMBO J* **3**, 665–670.
- Opstelten, D. J., de Groote, P., Horzinek, M. C., Vennema, H. & Rottier, P. J. (1993). Disulfide bonds in folding and transport of mouse hepatitis coronavirus glycoproteins. *J Virol* **67**, 7394–7401.
- Opstelten, D. J., Raamsman, M. J., Wolfs, K., Horzinek, M. C. & Rottier, P. J. (1995). Envelope glycoprotein interactions in coronavirus assembly. *J Cell Biol* **131**, 339–349.
- Peiris, J. S., Lai, S. T., Poon, L. L. & 14 other authors (2003). Coronavirus as a possible cause of severe acute respiratory syndrome. *Lancet* **361**, 1319–1325.
- Raamsman, M. J., Locker, J. K., de Hooge, A., de Vries, A. A., Griffiths, G., Vennema, H. & Rottier, P. J. (2000). Characterization of the coronavirus mouse hepatitis virus strain A59 small membrane protein E. *J Virol* **74**, 2333–2342.
- Simmons, G., Reeves, J. D., Rennekamp, A. J., Amberg, S. M., Piefer, A. J. & Bates, P. (2004). Characterization of severe acute respiratory syndrome-associated coronavirus (SARS-CoV) spike glycoprotein-mediated viral entry. *Proc Natl Acad Sci U S A* **101**, 4240–4245.
- Staropoli, I., Chanel, C., Girard, M. & Altmeyer, R. (2000). Processing, stability, and receptor binding properties of oligomeric envelope glycoprotein from a primary HIV-1 isolate. *J Biol Chem* **275**, 35137–35145.
- Stern, D. F. & Sefton, B. M. (1982). Coronavirus proteins: structure and function of the oligosaccharides of the avian infectious bronchitis virus glycoproteins. *J Virol* **44**, 804–812.
- Sui, J., Li, W., Murakami, A. & 11 other authors (2004). Potent neutralization of severe acute respiratory syndrome (SARS) coronavirus by a human mAb to S1 protein that blocks receptor association. *Proc Natl Acad Sci U S A* **101**, 2536–2541.
- Swift, A. M. & Machamer, C. E. (1991). A Golgi retention signal in a membrane-spanning domain of coronavirus E1 protein. *J Cell Biol* **115**, 19–30.
- Taguchi, F. (1993). Fusion formation by the uncleaved spike protein of murine coronavirus JHMV variant cl-2. *J Virol* **67**, 1195–1202.
- Taguchi, F., Ikeda, T., Saeki, K., Kubo, H. & Kikuchi, T. (1993). Fusogenic properties of uncleaved spike protein of murine coronavirus JHMV. *Adv Exp Med Biol* **342**, 171–175.
- Tripet, B., Howard, M. W., Jobling, M., Holmes, R. K., Holmes, K. V. & Hodges, R. S. (2004). Structural characterization of the SARS-coronavirus spike S fusion protein core. *J Biol Chem* **279**, 20836–20849.
- Tsang, K. W., Ho, P. L., Ooi, G. C. & 13 other authors (2003). A cluster of cases of severe acute respiratory syndrome in Hong Kong. *N Engl J Med* **348**, 1977–1985.
- Vennema, H., Godeke, G. J., Rossen, J. W., Voorhout, W. F., Horzinek, M. C., Opstelten, D. J. & Rottier, P. J. (1996). Nucleocapsid-independent assembly of coronavirus-like particles by co-expression of viral envelope protein genes. *EMBO J* **15**, 2020–2028.
- Wang, P., Chen, J., Zheng, A. & 15 other authors (2004). Expression cloning of functional receptor used by SARS coronavirus. *Biochem Biophys Res Commun* **315**, 439–444.
- Wei, X., Decker, J. M., Wang, S. & 12 other authors (2003). Antibody neutralization and escape by HIV-1. *Nature* **422**, 307–312.
- Williams, R. K., Jiang, G. S. & Holmes, K. V. (1991). Receptor for mouse hepatitis virus is a member of the carcinoembryonic antigen family of glycoproteins. *Proc Natl Acad Sci U S A* **88**, 5533–5536.
- Wong, S. K., Li, W., Moore, M. J., Choe, H. & Farzan, M. (2004). A 193-amino acid fragment of the SARS coronavirus S protein efficiently binds angiotensin-converting enzyme 2. *J Biol Chem* **279**, 3197–3201.
- Woo, P. C., Lau, S. K., Tsoi, H. W. & 11 other authors (2004). Relative rates of non-pneumonic SARS coronavirus infection and SARS coronavirus pneumonia. *Lancet* **363**, 841–845.
- Xiao, X., Chakraborti, S., Dimitrov, A. S., Gramatikoff, K. & Dimitrov, D. S. (2003). The SARS-CoV S glycoprotein: expression and functional characterization. *Biochem Biophys Res Commun* **312**, 1159–1164.
- Xiao, X., Feng, Y., Chakraborti, S. & Dimitrov, D. S. (2004). Oligomerization of the SARS-CoV S glycoprotein: dimerization of the N-terminus and trimerization of the ectodomain. *Biochem Biophys Res Commun* **322**, 93–99.
- Yang, T. T., Cheng, L. & Kain, S. R. (1996). Optimized codon usage and chromophore mutations provide enhanced sensitivity with the green fluorescent protein. *Nucleic Acids Res* **24**, 4592–4593.
- Yang, Z. Y., Kong, W. P., Huang, Y., Roberts, A., Murphy, B. R., Subbarao, K. & Nabel, G. J. (2004a). A DNA vaccine induces SARS coronavirus neutralization and protective immunity in mice. *Nature* **428**, 561–564.
- Yang, Z. Y., Huang, Y., Ganesh, L., Leung, K., Kong, W. P., Schwartz, O., Subbarao, K. & Nabel, G. J. (2004b). pH-dependent entry of severe acute respiratory syndrome coronavirus is mediated by the spike glycoprotein and enhanced by dendritic cell transfer through DC-SIGN. *J Virol* **78**, 5642–5650.
- Yeager, C. L., Ashmun, R. A., Williams, R. K., Cardellicchio, C. B., Shapiro, L. H., Look, A. T. & Holmes, K. V. (1992). Human aminopeptidase N is a receptor for human coronavirus 229E. *Nature* **357**, 420–422.
- Ying, W., Hao, Y., Zhang, Y. & 33 other authors (2004). Proteomic analysis on structural proteins of severe acute respiratory syndrome coronavirus. *Proteomics* **4**, 492–504.
- Yu, X., Bi, W., Weiss, S. R. & Leibowitz, J. L. (1994). Mouse hepatitis virus gene 5b protein is a new virion envelope protein. *Virology* **202**, 1018–1023.

